

Investigations of Local Pressure Drop Fluctuation Signals in Annular Type Fluidized Bed Photoreactor by Continuous Wavelet Transform

Wooseok Nam and Gui Young Han[†]

Department of Chemical Engineering, Sungkyunkwan University, Suwon 440-746, South Korea

(Received 21 February 2005 • accepted 22 June 2005)

Abstract—The wavelet transform is an effective tool for studying the dynamic behavior of fluidized beds in the resolution of time variables. To understand the behavior of photocatalyst under different velocity in an annular type fluidized bed, a new analysis technique (Continuous Wavelet Transform: CWT) is applied. With the time-frequency localization characteristics embedded in wavelets, the time and frequency information of signals can be presented as a visualized scheme. By analysis of various methods for pressure fluctuation signals measured from an annular type fluidized bed, it was found that the dynamic behavior of fluidization in the annulus fluidized bed reactor was easily observed with the aid of wavelet transform.

Key words: Fluidized Bed, Pressure Fluctuation, Continuous Wavelet Transform, Morlet Wavelet

INTRODUCTION

Fluidized beds have been applied in various industrial applications because of their desirable characteristics. A photoreactor using a fluidized bed not only brings higher contacting efficiency of photocatalysts and reactants but also enhances UV-light penetration through bubbles. Therefore, it is important to design a fluidized bed photoreactor having higher light throughputs, large treatment of reactants and lower pressure drop [Lim et al., 2002; Nam et al., 2002, 2004]. But heterogeneous flow patterns are not still clearly understood in fluidized beds. Various methods have been used for analyzing fluidized bed behavior, such as Fourier transform and fractal analysis. However, these methods do not contain local information of the signals. In 1982, Jean Morlet first introduced the idea of wavelets as a family of functions constructed by using translation and dilation of a single function, called the mother wavelet, for the analysis of signals [Morlet, 1982].

In this paper, a gas-solid phase fluidized bed photocatalytic oxidation system is designed to provide a surface of physical adsorption and photocatalytic oxidation of contaminant compounds into less a hazardous substance. The photocatalyst (TiO_2) is usually a fine powder phase (Geldart C type); the photocatalytic system must be followed with a fluid media-solid separation system. Especially, in gas phase fluidized bed photoreactor systems, fine photocatalysts are easily entrained from a fluidized bed reactor by up flow gas stream. Therefore, to provide a wide surface area and easy operation of a fluidized bed, the photocatalyst was loaded on a surface of silica gel [Kunii et al., 1991; Cheremishinoff et al., 1984].

The aim of the present work is to understand photocatalyst particle behavior under different velocity in an annular type fluidized bed. To do this, a new analysis technique (Continuous Wavelet Transform: CWT) was applied to investigate the local chaotic behavior of photocatalyst in the annulus regime of the bed.

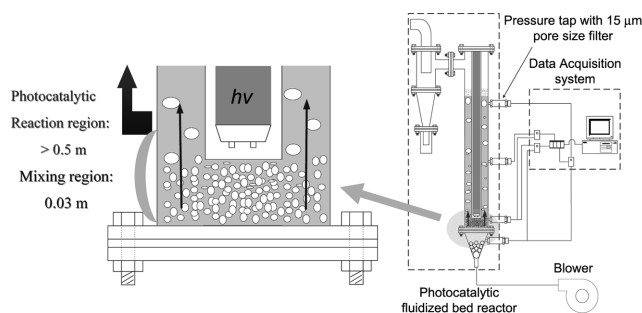


Fig. 1. Schematic diagram of experimental test set-up.

EXPERIMENTAL

The schematic diagram of experimental test set-up is shown in Fig. 1. The fluidized bed has an inside diameter of 0.06 m and 1.0 m long and is made of acrylic pipe. A 30 W UV-A Black Light lamp (BL) or 65 W low pressure mercury lamp (LPML, Sankyo Denki, Japan) was installed at the center of the reactor through the inside of the quartz tube of 0.03 m outside diameter and 1.0 m long. The inner quartz tube was located 0.03 m above the distributor as shown in Fig. 1; thus, a mixing zone was formed and it is expected that it will give space for better contacting between photocatalysts and gaseous pollutants. The $\text{TiO}_2/\text{SiO}_2$ photocatalysts employed are classified as B type in the Geldart Classification. In beds of Geldart B powder, bubbles form as soon as the gas velocity exceeds minimum fluidizing velocity (U_{mf}). The density of porous $\text{TiO}_2/\text{SiO}_2$ photocatalysts is 2.143 g/cm^3 and average particle diameter is about $130 \mu\text{m}$. Thus, these particles fluidize well with vigorous bubbling action and bubbles that grow large. The experimentally determined minimum fluidization velocity, U_{mf} was 0.67 cm/sec . Four pressure taps were installed vertically along the fluidized bed wall. The taps are connected to differential pressure transducers interfaced with a computer through the A/D converter for real-time data acquisition. Pressure drop data at four different bed heights, 0.01, 0.05

[†]To whom correspondence should be addressed.

E-mail: gyhan@skku.ac.kr

and 0.25 m above the distributor and 0.05 m below the distributor, were obtained. The signals of time series of the differential pressure fluctuations were sampled with a frequency of 100 Hz and the total acquisition time was 80 sec from 0.44 to 3.0 U_o/U_{mf} . Most of the experiments were repeated 5 times and similar results were collected.

1. Hurst Exponent

Hurst [1951] established rescaled range analysis by the non-dimensional H exponent, a statistical method to analyze long records of natural phenomena. By measures of the degree of freedom, he thought that could assume the changes occurred in the system.

A Hurst exponent (H) can assume any value between 0 and 1, and the points in a time series are uncorrelated when $H=0.5$. Processes with $0 < H < 0.5$ have a negative dependency structure and indicate persistence in the data, with the interval $0.5 < H < 1.0$ including positively dependent processes of 1/frequency and indicating anti-persistence in the data. If the Hurst exponent is 0.5, the phase is the perfect Brownian motion [Ellis et al., 2003; Vial et al., 2000].

2. Wavelet Transform (WT)

The Wavelet Transform (WT) can be used to analyze time-series that contain non-stationary power at many different frequencies [Daubechies, 1990]. Wavelet transforms are inner products of the signal and a family of the wavelet functions. According to a set of wavelet functions, WT can decompose the signal and translate it into a time-frequency domain through the translation and dilation processes.

3. Continuous Wavelet Transform (CWT)

Grossman and Morlet introduced the Continuous Wavelet Transform (CWT), which is a mathematical tool that can be used to decomposition, smoothing and denoising a signal in terms of elementary contributions called wavelets [Grossman et al., 1984]. The CWT $W_{\psi}f(a, b)$ the inner product of $f(t)$ with $\Psi_{a,b}(t)$, can be described by the equation

$$W_{\psi}f(a, b) = \frac{1}{\sqrt{a}} \int_{-\infty}^{\infty} f(t) \cdot \Psi\left(\frac{t-b}{a}\right) dt \quad (1)$$

Where $\Psi(t)$ is the Mother Wavelet, 'a' is the dilation parameter and

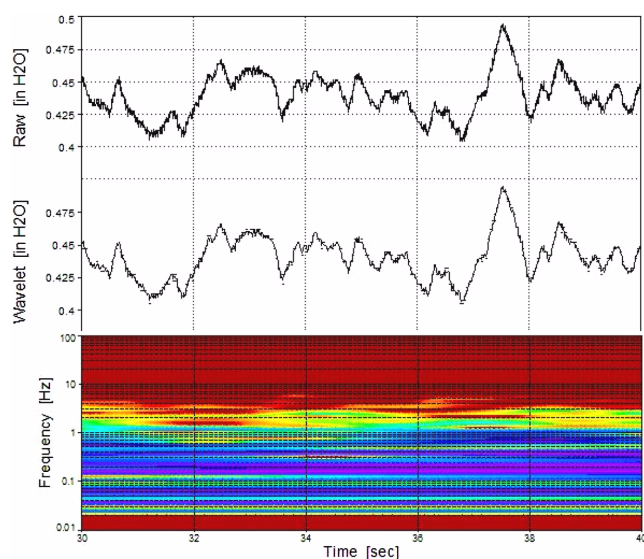


Fig. 2. Comparison of denoising plot by wavelet transform of raw data and rainbow spectrum plot of continuous wavelet transformed; $U_o/U_{mf}=0.44$ (0.6 L/min), $z=0.01$ m.

'b' the translation in time. The Wavelet basis function $\Psi_{a,b}(t)$ is a family of $\Psi(t)$ prototype functions. The signal was decomposed by using CWT of the computer program and analysis was done for the Morlet wavelet base [Torrence et al., 1998; Huang et al., 2001; Nikolaou et al., 2002; Park and Kim, 2001, 2003].

Fig. 2 is the procedure of wavelet denoising, reconstruction and spectrum plot of results of CWT. Pressure drop signals showed minor fluctuation due to noises. These noises can be eliminated by wavelet denoising. Fig. 2 also shows how Wavelet denoising is interpretable nearly in the original sign after the denoising step. A rainbow spectrum was obtained from the Continuous Wavelet Transform of pressure fluctuation signals with reconstruction to Wavelet denoising. The rainbow spectrum showed how the energy in the pressure fluctuation is distributed over both time and frequency: red regions represent low-energy values, and violet regions represent high-energy values.

RESULTS AND DISCUSSION

In a gas-solid fluidized bed, the main source of the pressure fluctuation signal originates from the formation of bubbles. As shown in Fig. 3, average absolute deviations (AAD) were presented with gas flow rate. The intensity of the signal can be measured and compared in a statistical method by using the AAD. It was observed that the AAD values increase with increasing gas velocity due to more bubble formation. For AAD values above the distributor, the increase of gas velocity beyond the 1.0 U_{mf} showed less effect on the AAD value of pressure fluctuation compared to the AAD value across the distributor. This is because the mixing zone between distributor and the bottom of the quartz tube in the bed acted as a buffer zone by compression of gas flow or cushion of pressure fluctuation. Such compressed gas flow infiltrates through the particles and thus the AAD value of pressure fluctuation is smaller.

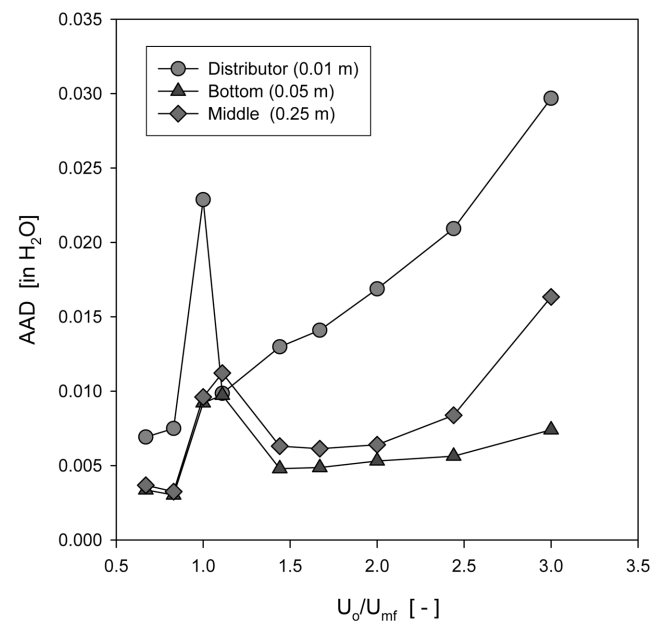


Fig. 3. Comparison of average absolute deviation (AAD) of pressure drop fluctuation signals in an annular fluidized bed with superficial gas velocity.

In this study, we compared the slope of the log-log plot of R/S vs. τ_H (H_1, H_2) at small time lags ($0 < \tau_H < 100$) and at large time lags ($100 < \tau_H < 1,000$), respectively. Following the original work of Hurst, the R/S method was used for the calculation of the scaling exponent (H ; Hurst exponent), to give quantitative information of the persistence of pressure drop fluctuation data. Common cases of fluctuation time records show a two slope R/S function separated by a breakpoint. As can be seen in Fig. 4, the slope of H_2 is smaller than 0.5, which it means that it is an anti-persistent behavior. Therefore,

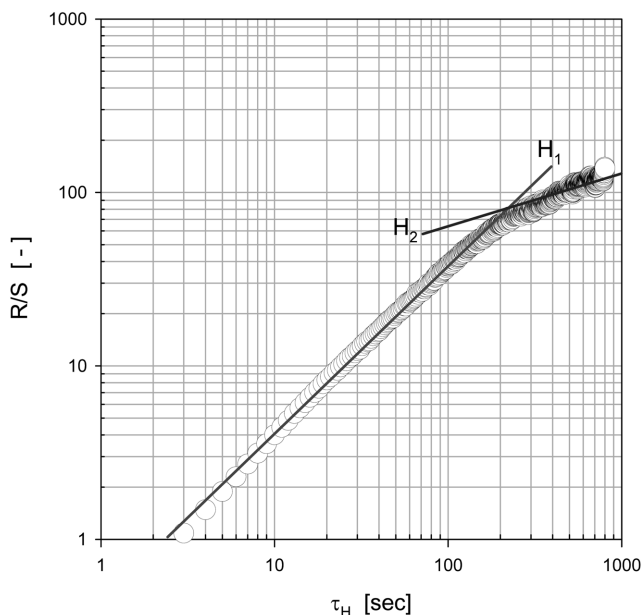


Fig. 4. Variation of rescaled range with time lags for fluctuation of pressure drop; $U_o/U_{mf}=3.0$ (2.7 L/min), $z=0.25$ m.

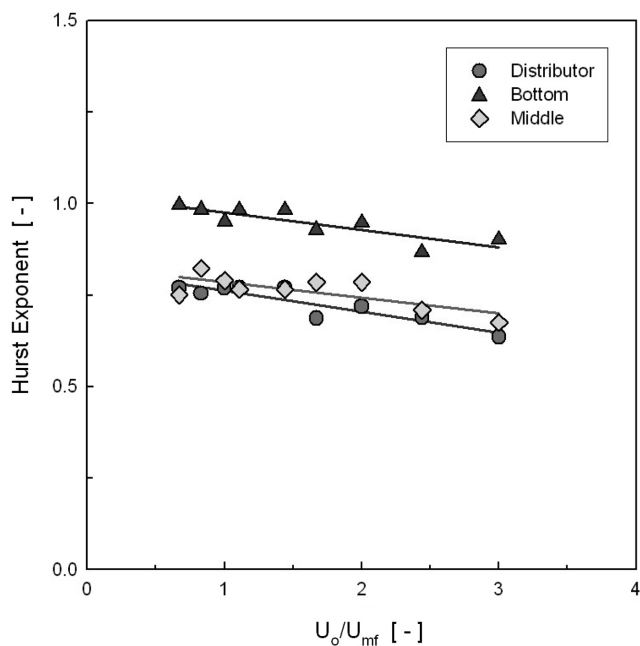


Fig. 5. Evolution of the Hurst exponents of the pressure drop fluctuation signals with superficial gas velocity.

we calculated the Hurst exponent at small time lags, H_1 . Fig. 5 shows the variations of Hurst exponents estimated from the pressure fluctuation signals with gas flow rates. The Hurst exponents decreased gradually with an increased gas flow rate in the annulus fluidized bed. For the annulus fluidized bed, the pressure fluctuation signals of the mixing zone exhibit a high persistence with Hurst exponent values close to unity. It indicated that the contact between gas and photocatalyst was not good enough in the bottom zone of the bed. However, with an increase of gas flow rate, the randomness is increased, which implies that the contact between the gas and photocatalysts gets better before photooxidation occurs. The gas hold-up also increased at the mixing zone.

Fig. 6 shows rainbow spectra plots of power, frequency vs. time-series for pressure drop fluctuations. A rainbow spectrum plot shows how the energy in the pressure fluctuation is distributed over both time and frequency (violet regions represent high-energy values, and red regions represent low-energy values). All spectra showed the wide ranges of frequencies, and most was low frequency. It is believed that this tendency was caused by the durable mechanical pulsation-energy of gas flow through the annular type fluidized bed. Fig. 6(a) and 6(b) show the pressure drop fluctuation below the minimum fluidization velocity condition. As shown in Fig. 6(a), and 6(b), since the gas flowed through the void of packed porous photocatalysts, high frequency and non-continuous spectra were obtained. It is considered that these weak spectra of pressure drop fluctuation signals were obtained as gas flow simply passed through narrow voids of packed photocatalysts. As gas velocity increased near to $1.0 U_{mf}$, the weak spectra of high frequency were diminished. From the minimum fluidization state (Fig. 6(c)), the weak spectra of high frequency disappeared, and the signals by motions of particles began to appear [Zhou et al., 2000; Ren et al., 2001]. Spectra of bubbles and dilute phases are presented by high frequency signals, and dense phases are presented by middle frequency signals individually. It was also observed that as the superficial gas velocity increased, the energies of middle and high frequencies spectra were more and more strengthened and pressure drop fluctuations by motions of individual dense phases and bubbles appeared. These pressure fluctuations were gradually delivered into the middle of the bed as the minimum fluidization (Fig. 6(c)) was begun. But, the relatively larger pressure drop fluctuations at the distributor were not delivered directly in the middle of the reactor because the mixing zone of bottom of the bed acts a buffer zone. As shown in Fig. 6(e)-6(i), the energies of bubbles spectra and clusters were stronger with the increase of superficial gas velocities. It is believed that these tendencies show vigorous mixing of gases and photocatalyst expanding to the whole bed with the increase of gas velocity.

CONCLUSION

By the continuous wavelet transform analysis of pressure fluctuation signals measured from an annular type fluidized bed, it was observed that pressure drop fluctuation of the whole bed was smaller than that of the distributor because the mixing zone acts as a buffer zone placed above the distributor.

Continuous wavelet transform is an effective method for monitoring the dynamics of pressure fluctuation of bubbles as time varies in an annular type fluidized bed photoreactor. Also, the transition

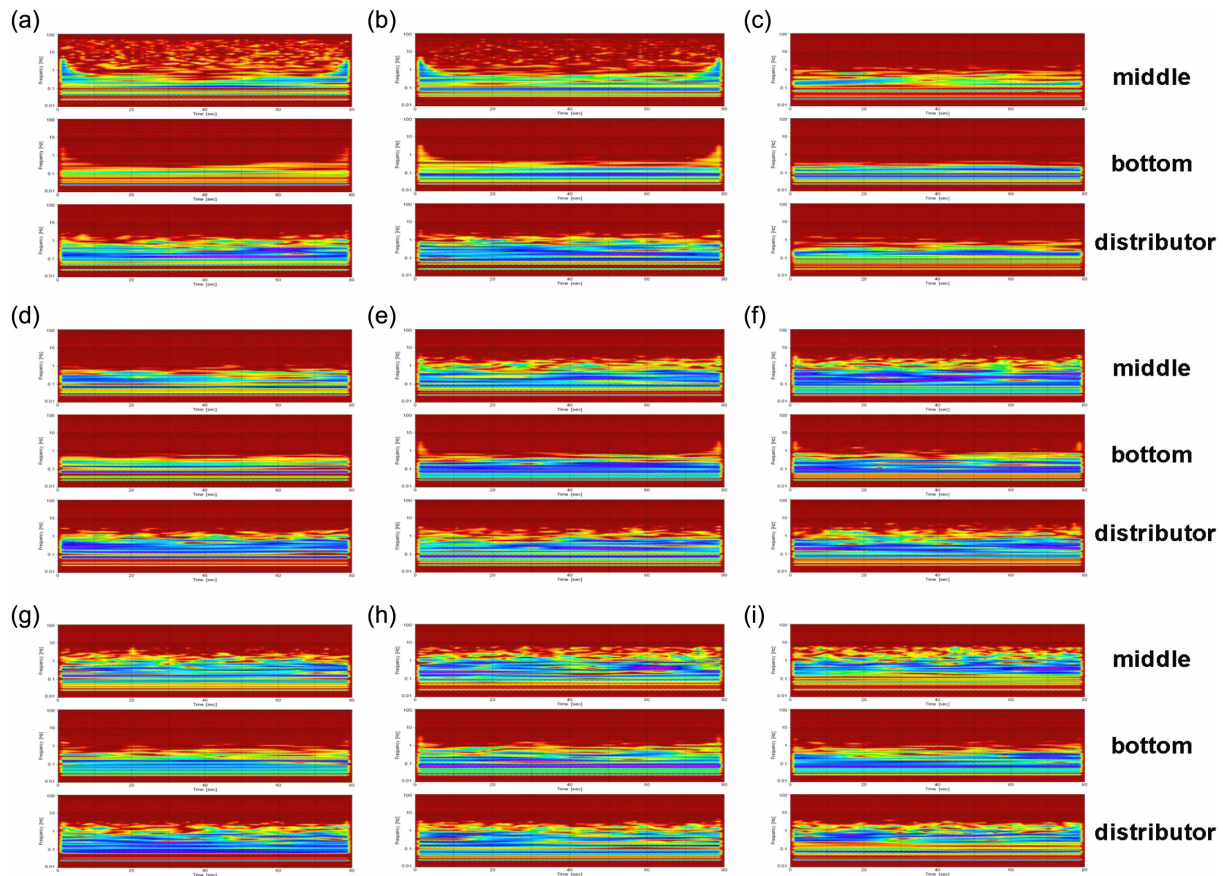


Fig. 6. A rainbow spectrum plot of how the energy in the pressure drop fluctuation is distributed over both time and frequency; violet regions represent high-energy values, and red regions represent low-energy values; (a)= $0.67 U_{mf}$, (b)= $0.83 U_{mf}$, (c)= $1.00 U_{mf}$, (d)= $1.11 U_{mf}$, (e)= $1.44 U_{mf}$, (f)= $1.67 U_{mf}$, (g)= $2.00 U_{mf}$, (h)= $2.44 U_{mf}$ and (i)= $3.00 U_{mf}$.

of fluidization regimes in the annulus fluidized bed reactor with gas velocity was easily observed with the aid of wavelet transform.

ACKNOWLEDGMENT

This work was supported by grant No. R01-2004-000-10028-0 from the Basic Research Program of the Korea Science and Engineering Foundation.

NOMENCLATURE

- a : the dilation parameter [-]
 b : the translation in time [-]
 H, H_1, H_2 : Hurst exponent [-]
 R/S : rescaled range analysis [-]
 U_o : superficial gas velocity [cm/sec]
 U_{mf} : minimum fluidization velocity [cm/sec]
 $W_{\psi}f(a, b)$: continuous wavelet transform function [-]

Greek Letters

- τ_H : time lag [sec]
 Ψ : mother wavelet [-]
 $\Psi_{a,b}(t)$: wavelet basis function [-]

REFERENCES

- Cheremishinoff, N. P. and Cheremishinoff, P. N., *Hydrodynamics of Gas-Solids Fluidization*, Gulf Publishing Company, Houston, 137 (1984).
 Daubechies, I., "The Wavelet Transform Time-frequency Localization and Signal Analysis," *IEEE Trans. Inform. Theory*, **36**, 961 (1990).
 Ellis, N., Briens, L. A., Grace, J. R., Bi, H. T. and Lim, C. J., "Characterization of Dynamic Behavior in Gas-solid Turbulent Fluidized Bed using Chaos and Wavelet Analyses," *Chem. Eng. J.*, **96**, 105 (2003).
 Farge, M., "Wavelet Transforms and Their Applications to Turbulence," *Annu. Rev. Fluid Mech.*, **24**, 395 (1992).
 Grossman, A. and Morlet, J., "Decomposition of Hardy Functions into Square Integrable Wavelets of Constant Shape," *SIAM J. Math. Anal.*, **15**, 723 (1984).
 Huang, S. and Hsieh, C., "Visualizing Time-varying Power System Harmonics using a Morlet Wavelet Transform Approach," *Electric Power Systems Research*, **58**, 81 (2001).
 Hurst, H. E., "Methods of using Long-term Storage in Reservoirs," *Trans. Amer. Soc. Civil Engrs.*, **116**, 770 (1951).
 Kim, M. J., Nam, W. and Han, G. Y., "Photocatalytic Oxidation of Ethyl Alcohol in an Annulus Fluidized Bed Reactor," *Korean J. Chem. Eng.*, **21**, 721 (2004).
 Kunii, D. and Levenspiel, O., *Fluidization Engineering*, Butterworth-Heinemann, Boston, 71 (1991).
 Lim, T. H. and Kim, S. D., "Photocatalytic Degradation of Trichloroethylene over TiO_2/SiO_2 in an Annulus Fluidized Bed Reactor," *Korean J. Chem. Eng.* (Vol. 22, No. 6)

- J. Chem. Eng.*, **19**, 1072 (2002).
- Morlet, J., Arens, G., Fourgeau, E. and Glard, D., "Wave Propagation and Sampling Theory-Part I: Complex Signal and Scattering in Multilayered Media," *Geophysics*, **47**, 203 (1982).
- Nam, W., Kim, J. and Han, G. Y., "Photocatalytic Oxidation of Methyl Orange in a Three-phase Fluidized Bed Reactor," *Chemosphere*, **47**, 1019 (2002).
- Nikolaou, N. G. and Antoniadis, I. A., "Demodulation of Vibration Signals Generated by Defects in Rolling Element Bearings using Complex Shifted Morlet Wavelets," *Mech. Sys. and Signal Proc.*, **16**, 677 (2002).
- Park, S. H. and Kim, S. D., "Characterization of Pressure Signals in a Bubble Column by Wavelet Packet Transform," *Korean J. Chem. Eng.*, **20**, 128 (2003).
- Park, S. H. and Kim, S. D., "Wavelet Transform Analysis of Pressure Fluctuation Signals in a Three-Phase Fluidized Bed," *Korean J. Chem. Eng.*, **18**, 1015 (2001).
- Ren, J., Mao, Q., Li, J. and Lin, W., "Wavelet Analysis of Dynamic Behavior in Fluidized Beds," *Chem. Eng. Sci.*, **56**, 981 (2001).
- Torrence, C. and Compo, G. P., "A Practical Guide to Wavelet Analysis," *Bull. Amer. Meteor. Soc.*, **79**, 61 (1998).
- Vial, C., Camarasa, E., Poncin, S., Wild, G., Midox, N. and Bouillard, J., "Study of Hydrodynamic Behavior in Bubble Columns and External Loop Airlift Reactors through Analysis of Pressure Fluctuations," *Chem. Eng. Sci.*, **55**, 2957 (2000).
- Zhou, H., Lu, H. and Lin, L., "Turbulence Structure of the Solid Phase in Transition Region of a Circulating Fluidized Bed," *Chem. Eng. Sci.*, **55**, 839 (2000).